



RESEARCH MEMORANDUM

LOW-SPEED LONGITUDINAL AERODYNAMIC CHARACTERISTICS OF A
 45° SWEPTBACK WING WITH DOUBLE SLOTTED FLAPS

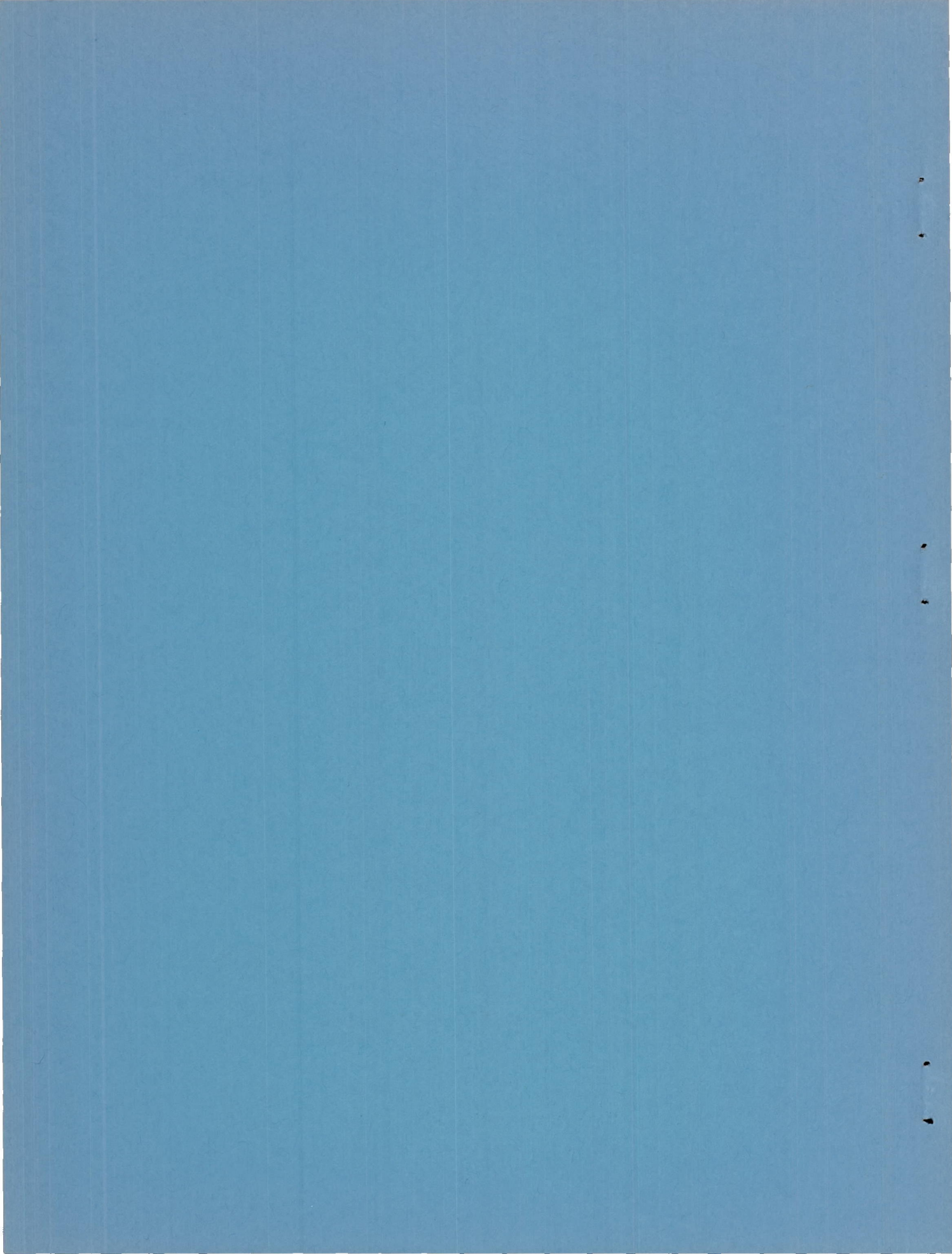
By Rodger L. Naeseth

Langley Aeronautical Laboratory
Langley Field, Va.

NATIONAL ADVISORY COMMITTEE
FOR AERONAUTICS

WASHINGTON

April 10, 1956
Declassified March 11, 1957



NATIONAL ADVISORY COMMITTEE FOR AERONAUTICS

RESEARCH MEMORANDUM

LOW-SPEED LONGITUDINAL AERODYNAMIC CHARACTERISTICS OF A
 45° SWEPTBACK WING WITH DOUBLE SLOTTED FLAPS

By Rodger L. Naeseth

SUMMARY

A low-speed investigation has been made to determine the effect of double slotted flaps consisting of a 0.213-wing-chord main flap and either a 0.500-flap-chord vane or a 0.266-flap-chord vane on the aerodynamic characteristics of a 45° sweptback wing. The flap had a span of 0.35 wing semispan with the inboard end at 0.16 semispan. The wing had an aspect ratio of 3.7, a taper ratio of 0.41, symmetrical sections, and an average streamwise thickness ratio of 0.086. The test Reynolds number was 1.8×10^6 , based on the wing mean aerodynamic chord.

The double slotted flaps maintained effectiveness to high flap-deflection angles and, at an angle of attack of 0° , produced lift-coefficient increments of 0.67 at a flap deflection of 80° for the configuration with the 0.500-flap-chord vane and 0.55 at a flap deflection of 66° for the flap with the 0.266-flap-chord vane.

The stall of the two double-slotted-flap configurations occurred at an angle of attack which was about one-half the angle of attack at which the plain wing stalled and resulted in a maximum lift coefficient for the flapped configurations which was about 0.15 higher than the maximum lift coefficient of 1.02 attained by the plain wing. The maximum lift coefficients of the double-slotted-flap configurations were about the same.

For comparison with the double slotted flaps, either or both of the slots in the flaps were blocked and faired, thus simulating single slotted flaps or extended plain flaps. The results indicated that, at moderate flap deflections and angles of attack, blocking the slots increased the lift effectiveness slightly; however, the blocked flaps lost effectiveness at lower flap deflections than the slotted flaps with the consequence that the maximum lift obtained was somewhat lower than the maximum lift obtained for the double slotted flaps.

INTRODUCTION

An investigation is being made by the National Advisory Committee for Aeronautics to study the characteristics of various high-lift devices on a full-scale 45° sweptback wing. One-fifth scale tests of the double-slotted-flap designs proposed for tests at full scale were made in the Langley 300 MPH 7- by 10-foot tunnel to determine the effect of the flaps on the longitudinal aerodynamic characteristics of the sweptback wing. The wing had an aspect ratio of 3.7, symmetrical sections, a taper ratio of 0.41, and an average streamwise thickness ratio of 0.086.

In order that the design of the double slotted flaps developed in the small-scale tests can be used in the full-scale tests, the same span of flap (0.35 semispan) and the same forward limit of space for retraction (0.735 wing chord line) were used. Two double-slotted-flap configurations were used. For one, a ratio of vane chord to flap chord of one-half was chosen because it was shown to be optimum in a summary of existing two-dimensional data (ref. 1). The flap, rearward of the vane, was 0.213 wing chord. For the other design, a smaller vane (0.266 flap chord), fixed to the flap, was chosen because it would require a less complicated retracting mechanism.

For comparison with the double-slotted-flap characteristics, the characteristics of a single-slotted-flap arrangement and an extended plain flap were obtained. The single slotted flap was simulated by blocking either of the slots, and the extended plain flap by blocking both slots.

SYMBOLS

The forces and moments measured on the wing are presented about the wind axes which, for the conditions of these tests (zero sideslip), correspond to the stability axes. The pitching-moment data are measured about the origin of axes as shown in figure 1 which corresponds to the 25-percent-chord station of the mean aerodynamic chord. The lift, drag, and pitching-moment data presented herein represent the aerodynamic effects of deflection of the flaps in the same direction on both semi-spans of the complete wing.

C_L lift coefficient, F_L/qS

ΔC_L increment of lift coefficient

C_D drag coefficient, F_D/qS

$C_{m,w}$	pitching-moment coefficient, $M_{Yw}/qS\bar{c}$
F_L	twice lift of semispan model, lb
F_D	twice drag of semispan model, lb
M_{Yw}	twice pitching moment of semispan model measured about 0.25 \bar{c} , ft/lb
q	free-stream dynamic pressure, $\rho V^2/2$, lb/sq ft
S	twice wing area of semispan model, sq ft
\bar{c}	mean aerodynamic chord of wing, ft
c	local chord, ft
b	wing span, ft
V	free-stream velocity, ft/sec
ρ	mass density of air, slugs/cu ft
α	angle of attack of wing, deg
δ_f	flap deflection relative to wing chord plane, measured in a plane normal to a line swept back 36.77° (positive when trailing edge is down), deg

Subscripts:

f	flap
Λ	normal to a line swept back 36.77°

MODEL AND APPARATUS

The model-wing geometry is given in figure 1. The wing was of aspect ratio 3.7 and taper ratio 0.41 and had symmetrical airfoil sections. Leading-edge sweep was 47.8° and the wing had no geometric dihedral or twist. The percent-thickness ratio of the wing in a streamwise direction varied from 8.3 at the root to 9.0 at the tip. The test wing was a 1/5-size model of a wing on which a general investigation of high-lift devices is in progress. The model wing was derived in the same manner as the full-scale wing in that the sweep of an existing wing was increased

and the plan form was further altered by reducing the sweep of the wing trailing edge and fairing the sections to the revised trailing edge with straight lines. The resulting airfoil sections at the two spanwise stations shown in figure 1 are given in table I.

The direction in which the flap ends were cut, the forward limit of space available for flap retraction, 0.735 chord line, and the span of flap, $0.160\frac{b}{2}$ to $0.507\frac{b}{2}$, were determined by the structure of the full-scale wing. The double-slotted flap arrangement (fig. 2) consisted of a $0.213c$ main flap in combination with a $0.500c_f$ vane and also with a $0.266c_f$ vane (streamwise values). The coordinates of the flap ends are given in table II. Both of these configurations were capable of being retracted into the designated space in the wing. The $0.500c_f$ vane was chosen because it was shown to be the optimum in a summary of two-dimensional results, (ref. 1); and the $0.266c_f$ vane was the largest vane which could be retracted into the designated space without relative movement between vane and flap. St Cyr 156 sections, reference 2, were used for the vanes because the rounded leading edge of the section allows deflection of the vane-flap assembly as a unit about a fixed pivot through a large angle range while maintaining a desirable lip and vane relationship, figure 2; also the sections remain unstalled over a large angle-of-attack range. The flap-deflection angles were measured in the plane of the flap ends, that is, normal to a line swept 36.77° .

Provision was made for minor changes in the flap geometry. The flap and $0.500c_f$ vane assembly pivot point could be moved forward a distance of $0.024c_{f,\Lambda}$, and down a distance of $0.012c_{f,\Lambda}$, (fig. 3(a)), or the flap part could be moved forward along its chord plane relative to the vane a distance of $0.062c_{f,\Lambda}$, (fig. 3(b)). The lower surface wing lip was removable. Filler blocks of balsa wood were provided to block the slots (fig. 4).

The wing was aluminum except for the trailing-edge modification mentioned previously and the flap, both of which were made of mahogany reinforced with an aluminum plate extending to the trailing edge. The vanes were machined from aluminum. The larger of the vanes was supported at each end, the smaller vane required a center support in addition to the end supports.

The semispan-wing model was mounted vertically in the Langley 300 MPH 7- by 10-foot tunnel. The root chord of the model was adjacent to the ceiling of the tunnel which served as a reflection plane. A small clearance was maintained between the model and the tunnel ceiling so that no part of the model came into contact with the tunnel structure. In order to minimize the effect of spanwise air flow over the model through this clearance hole, a $1/16$ -inch-thick metal end plate, which projected about 1 inch above the wing surface, was attached to the root of the model.

TESTS AND CORRECTIONS

Description of Tests

Data were obtained through an angle-of-attack range of -6° to 26° for all configurations and the flap-deflection range extended to 80.4° . The configurations tested and flap-deflection ranges are summarized in table III.

The tests were performed at an average dynamic pressure of approximately 25.4 pounds per square foot, which corresponds to a Mach number of 0.13 and a Reynolds number of 1.8×10^6 based on the wing mean aerodynamic chord.

Corrections

Jet-boundary corrections, determined by the method presented in reference 3 have been applied to the angle-of-attack and the drag coefficient values. Blocking corrections, to account for the constriction effects of the model and its wake have also been applied to the test data. The blocking corrections were computed by the method of reference 4.

RESULTS AND DISCUSSION

Presentation of Results

The lift, drag, and pitching-moment characteristics are presented for the wing and flap with the $0.500c_f$ vane in figures 5 to 9 and for the wing and flap with the $0.266c_f$ vane in figures 10 to 13. Characteristics of the plain wing are included in each figure. Figures 14 to 17 are summaries of the lift increment for the range of flap deflections tested and are given for angles of attack of 0° , 4° , and 10° .

Lift Characteristics

Plain wing.— Plain-wing results show a lift-curve slope of 0.053 at $\alpha = 0^\circ$. The lift-curve slope begins to increase at $C_L \approx 0.30$ and appears typical of swept wings having leading-edge-separation-vortex-type flow. The maximum lift coefficient was 1.02 and was obtained at an angle of attack of 24° .

Flap with 0.500cf vane.- The results for the wing with double slotted flaps with the 0.500cf vane, figure 5, indicated a lift coefficient increment at $\alpha = 0^\circ$ of 0.67 obtained with $\delta_f = 80.4^\circ$; however the stall of the flapped wing occurred at about 12° angle of attack, much lower than the plain wing which had maximum C_L at $\alpha = 24^\circ$, and resulted, therefore, in a maximum lift coefficient for the flapped configuration which was about 0.15 higher than the maximum lift coefficient of 1.02 attained by the plain wing.

For comparison with the double slotted flap the characteristics of a single slotted flap and extended plain flap were obtained. The single slotted flap was simulated by blocking either of the slots and the extended plain flap by blocking both slots. The results, figures 6 to 8, show a similar variation of lift coefficient with angle of attack for these configurations as compared to the double slotted flap. When both slots were blocked, figure 8, the curves for $\delta_f = 65.4^\circ$ and 70.7° show a sharp loss in lift above $\alpha = 0^\circ$. A similar result occurred with the rear slot blocked (fig. 6).

The increments of lift coefficient for the double slotted flaps and various modifications are compared in figures 14 and 15 at three angles of attack. At $\alpha = 0^\circ$ the double-slotted-flap-lift increment increased with deflection through the maximum angle tested, 80.4° , where ΔC_L was 0.67. At $\alpha = 10^\circ$ this maximum increment had decreased to 0.58 and was obtained with a flap deflection of 75.6° . Blocking of either or both of the slots resulted in an increase in ΔC_L at the lower flap deflections; however, earlier stall as the flap deflections were increased limited the maximum ΔC_L attained by the flaps with either or both slots blocked to values somewhat less than those of the double slotted flap. This difference between the maximum ΔC_L for the double slotted flap and the flaps with one or both slots blocked was small (generally less than 0.04) throughout the angle-of-attack range except that at $\alpha = 4^\circ$ the maximum ΔC_L for the flap with both slots blocked was about 0.08 lower than the maximum value of ΔC_L of the double slotted flap.

Some flow studies were made to check the effectiveness of the slots in controlling the flow over the double slotted flaps and to explain the result that the flap with slots blocked maintained effectiveness to higher deflection angles than expected. Observation of tufts on the flap indicated that up to $\alpha = 12.7^\circ$ (the highest angle of the tuft tests) the slots were effective in maintaining smooth flow over the double slotted flap to the highest deflection tested, 80.4° , and that unsteady flow existed on the flap with slots blocked over the angle-of-attack and flap-deflection ranges investigated. Observation of a single tuft on a probe indicated that a vortex-type flow existed over the inboard part of the flaps with slots blocked. The existence of this flow offers a possible

explanation of the ability of the flap with slots blocked to maintain effectiveness to high deflection angles.

As shown in figure 15, either moving the flap forward relative to the vane or moving the pivot point on the wing had only a small effect on the lift available.

Flap and $0.266c_f$ vane. - The effects of the flap with the $0.266c_f$ vane on the wing characteristics through the angle-of-attack range were similar to the effects of the larger vane and flap (fig. 10). Lift increments at $\alpha = 0^\circ$ were less for the small vane configuration than for the large vane configuration, however the maximum lift is nearly as high. Although the limited number of deflections tested do not define the variation of ΔC_L with δ_f , it appears that blocking either or both of the slots generally resulted in slightly higher maximum ΔC_L than for the double slotted flap at the angles of attack and deflection range shown in figure 16.

Increasing the vane size (fig. 17) from $0.266c_f$ to $0.500c_f$ resulted in greater ΔC_L over the angle-of-attack and deflection ranges. At $\alpha = 0^\circ$ the maximum ΔC_L was 0.67 at $\delta_f = 80.4^\circ$ for the double slotted flap ($0.500c_f$ vane) compared with 0.55 at $\delta_f = 66^\circ$ for the smaller vane and flap.

Comparison with theory. - Values of the increment of lift theoretically obtainable by a $0.213c$ plain flap also are presented in figure 17 for comparison with the experimental results. These values were computed by use of reference 5, which was modified with an aspect ratio correction to the flap effectiveness factor by the method described in reference 6. These values were for streamwise deflections and therefore the deflections were converted to the corresponding deflections parallel to the flap ends for presentation on figure 17. As shown in the figure, the values of lift increment obtained experimentally are lower than theoretical values. Similar results for the two-dimensional case are shown in reference 1, in which it is concluded that some form of forced boundary-layer control is required to obtain or exceed theoretically obtainable values.

Pitching-Moment Characteristics

Pitching-moment characteristics of the plain wing, figure 5, indicated an increasingly stable variation of pitching moment with lift coefficient to $C_L = 0.6$. The unstable break in the curve occurred at $C_L = 0.80$. The aerodynamic center was located at approximately $0.28c$ at low angles of attack. The addition of the double slotted flap

(0.500cf vane) or its various modifications resulted in a small rearward shift of the aerodynamic center, a delay in the unstable break of the pitching-moment curve to $C_L = 1.0$, and, for example, at $\delta_f = 50.7^\circ$ a $C_{m,w}$ increment of about -0.13. The pitching-moment results for the flap with both slots blocked (fig. 8) were somewhat irregular as compared to the double slotted flap at the lower deflections; and at flap deflections of about 65° and greater, the marked changes in the lift curves discussed previously had correspondingly large changes in $C_{m,w}$ (about 0.05 decrease in $C_{m,w}$ between $\alpha = 0^\circ$ and $\alpha = 2^\circ$). A similar effect is shown in figure 6 for the flap with rear slot blocked.

Generally the same trends were shown for the flap and small vane (figs. 10 to 13), except that the unstable break in the pitching-moment-coefficient curve occurs at a lower lift coefficient than for the flap and large vane.

Drag Characteristics

Analysis of the lift and drag data indicates that, for lift coefficients in the range just below stall, a flap deflection of about 50° provides the highest value of lift-drag ratio (about 3.9). Further increases in flap deflection generally result in a decrease in lift-drag ratio. Therefore an advantage may be gained by limiting the flap deflections. When high drag coefficients are desirable to increase the glide-path angle or when a lower angle of attack is desirable, higher angles of deflection may be used. Lift-drag ratios for the various flaps showed little difference at these high-lift coefficients.

CONCLUDING REMARKS

A low-speed investigation has been made to determine the effect of double slotted flaps consisting of a 0.213-wing-chord main flap and either a 0.500-flap-chord vane or a 0.266-flap-chord vane on the aerodynamic characteristics of a 45° sweptback wing. The wing had an aspect ratio of 3.7, a taper ratio of 0.41, and an average thickness ratio of 0.086. The test Reynolds number was 1.8×10^6 , based on the mean aerodynamic chord.

The double slotted flaps maintained effectiveness to high flap deflections and, at an angle of attack of 0° , produced lift-coefficient increments of 0.67 at a flap deflection of about 80° for the flap with 0.500-flap-chord vane and 0.55 at a flap deflection of about 66° for the flap with the 0.266-flap-chord vane. The stall of the two double-slotted-flap configurations occurred at an angle of attack which was about one-half

the angle of attack at which the plain wing stalled and resulted in a maximum lift coefficient for the flapped configurations which was about 0.15 higher than the maximum lift coefficient of 1.02 attained by the plain wing. The maximum lift coefficients of the two flapped configurations were about the same.

For comparison with the double slotted flaps, slots in the flaps were blocked and faired thus simulating single slotted flaps or extended plain flaps. The results indicated that, at moderate flap deflections and angles of attack, blocking either or both of the slots increased the lift effectiveness slightly; however, the blocked flaps lost effectiveness at lower flap deflections than the slotted flaps with the consequence that the maximum lift obtained was somewhat lower than the maximum lift obtained for the double slotted flaps.

Langley Aeronautical Laboratory,
National Advisory Committee for Aeronautics,
Langley Field, Va., December 21, 1955.

REFERENCES

1. Riebe, John M.: A Correlation of Two-Dimensional Data on Lift Coefficient Available With Blowing-, Suction-, Slotted-, and Plain-Flap High-Lift Devices. NACA RM L55D29a, 1955.
2. National Advisory Committee for Aeronautics: Aerodynamic Characteristics of Airfoils. NACA Rep. 315, 1929.
3. Gillis, Clarence L., Polhamus, Edward C., and Gray, Joseph L., Jr.: Charts for Determining Jet-Boundary Corrections for Complete Models in 7- by 10-Foot Closed Rectangular Wind Tunnels. NACA WR L-123, 1945. (Formerly NACA ARR L5G31.)
4. Herriot, John G.: Blockage Corrections for Three-Dimensional-Flow Closed-Throat Wind Tunnels, With Consideration of the Effect of Compressibility. NACA Rep. 995, 1950. (Supersedes NACA RM A7B28.)
5. DeYoung, John.: Theoretical Symmetric Span Loading Due to Flap Deflection for Wings of Arbitrary Plan Form at Subsonic Speeds. NACA Rep. 1071, 1952. (Supersedes NACA TN 2278.)
6. Swanson, Robert S., and Crandall, Stewart M.: Lifting-Surface-Theory Aspect-Ratio Corrections to the Lift and Hinge-Moment Parameters for Full-Span Elevators on Horizontal Tail Surfaces. NACA Rep. 911, 1948. (Supersedes NACA TN 1175.)

TABLE I
 COORDINATES OF THE SYMMETRICAL WING AT
 SPANWISE STATIONS 1 AND 2
 [Coordinates in percent wing chord]

Station 1; chord, 20.613 in.		Station 2; chord, 15.771 in.	
Station	Ordinate	Station	Ordinate
0	0	0	0
.44	.82	.45	.84
.66	.99	.68	1.01
1.11	1.23	1.13	1.26
2.22	1.67	2.27	1.71
4.44	2.32	4.53	2.37
6.66	2.84	6.80	2.90
8.89	3.26	9.08	3.33
13.34	3.93	13.62	4.01
17.80	4.45	18.18	4.54
22.27	4.84	22.74	4.95
26.75	5.12	27.30	5.23
31.22	5.30	31.87	5.42
35.71	5.38	36.46	5.50
40.20	5.34	41.04	5.45
44.70	5.18	45.63	5.28
49.20	4.87	50.23	4.97
60.30	3.81	63.20	3.92
68.92	2.77	70.51	3.11
^a 74.07	2.12	^a 74.52	2.60
80.87	1.59	81.21	1.95
87.66	1.06	87.89	1.29
94.45	.53	94.57	.63
100.00	.10	100.00	.10

^aStraight line to trailing edge.

TABLE II

COORDINATES OF THE FLAP ENDS

[All values in percent flap chord]

Station	Inboard ordinate		Station	Outboard ordinate	
	Upper surface	Lower surface		Upper surface	Lower surface
0	-5.43	5.43	0	-6.99	6.99
1.45	-2.83	6.81	1.88	-3.82	8.62
2.79	-1.65	7.31	3.42	-2.48	9.12
5.47	0	7.46	6.49	-0.59	9.27
8.08	1.11	7.42	9.62	.84	9.17
10.72	2.10	7.39	12.69	2.03	9.02
15.96	3.75	6.97	18.74	4.11	8.38
21.16	4.75	6.58	24.83	5.40	7.78
31.69	5.66	5.78	36.98	6.39	6.59
42.10	4.98	4.94	49.12	5.40	5.35
52.16	4.17	4.17	53.09	5.06	5.06
78.55	2.09	2.09	79.08	2.48	2.48
100.00	.38	.38	100.00	.40	.40

TABLE III
CONFIGURATIONS TESTED

Flap arrangement	Figure		Deflections tested, deg
	Geometry	Data	
Flap and $0.50c_f$ vane:			
Double slotted	2(a)	5	45.7 to 80.4
Rear slot blocked	4(b)	6	50.7 to 80.4
Forward slot blocked	4(c)	7	40.7 to 80.4
Slots blocked	4(a)	8	40.7 to 75.6
Double slotted with flap part moved forward	3(b)	9	51.1 and 70.9
Double slotted with pivot moved forward and down	3(a)	9	70.2 and 81.9
Flap and $0.266c_f$ vane:			
Double slotted	2(b)	10	31.0 to 70.9
Rear slot blocked	4(b)	11	31.0, 50.9, 70.9
Rear slot blocked and lower lip off	- - -	11	50.9 and 70.9
Forward slot blocked	4(c)	12	50.9 and 70.9
Slots blocked	4(a)	13	31.0 to 70.9

Wing -

Sweep

C/4 line	44.62°
reference line	45.00°
Aspect ratio	3.7
Taper ratio	.41
Area of semispan \bar{c}	6.82 sq.ft. 2.053 ft

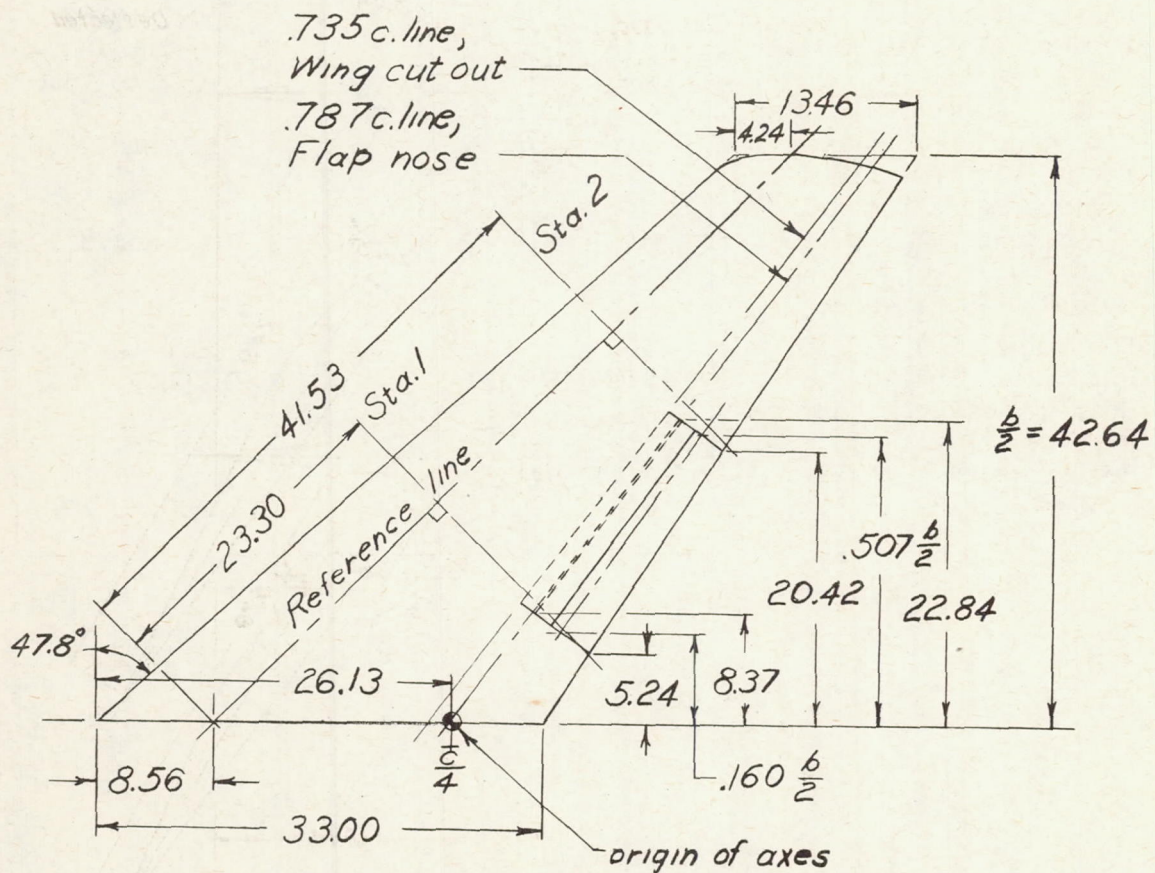


Figure 1.- Geometric characteristics of the model. All dimensions are in inches except as noted.

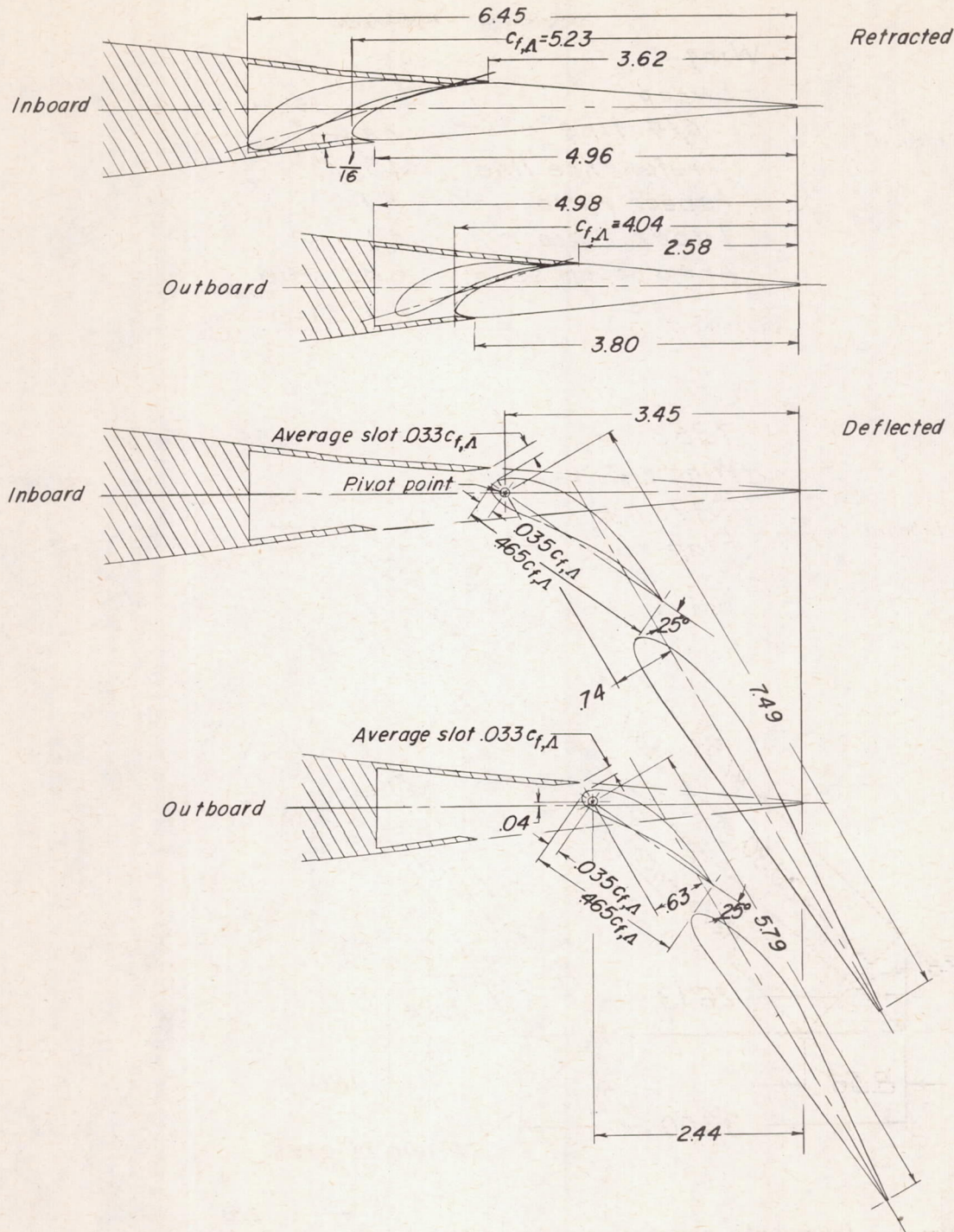
(a) Flap and $0.500c_f$ vane.

Figure 2.- Sections of double-slotted flaps in planes of flap ends. Dimensions given in inches except where noted.

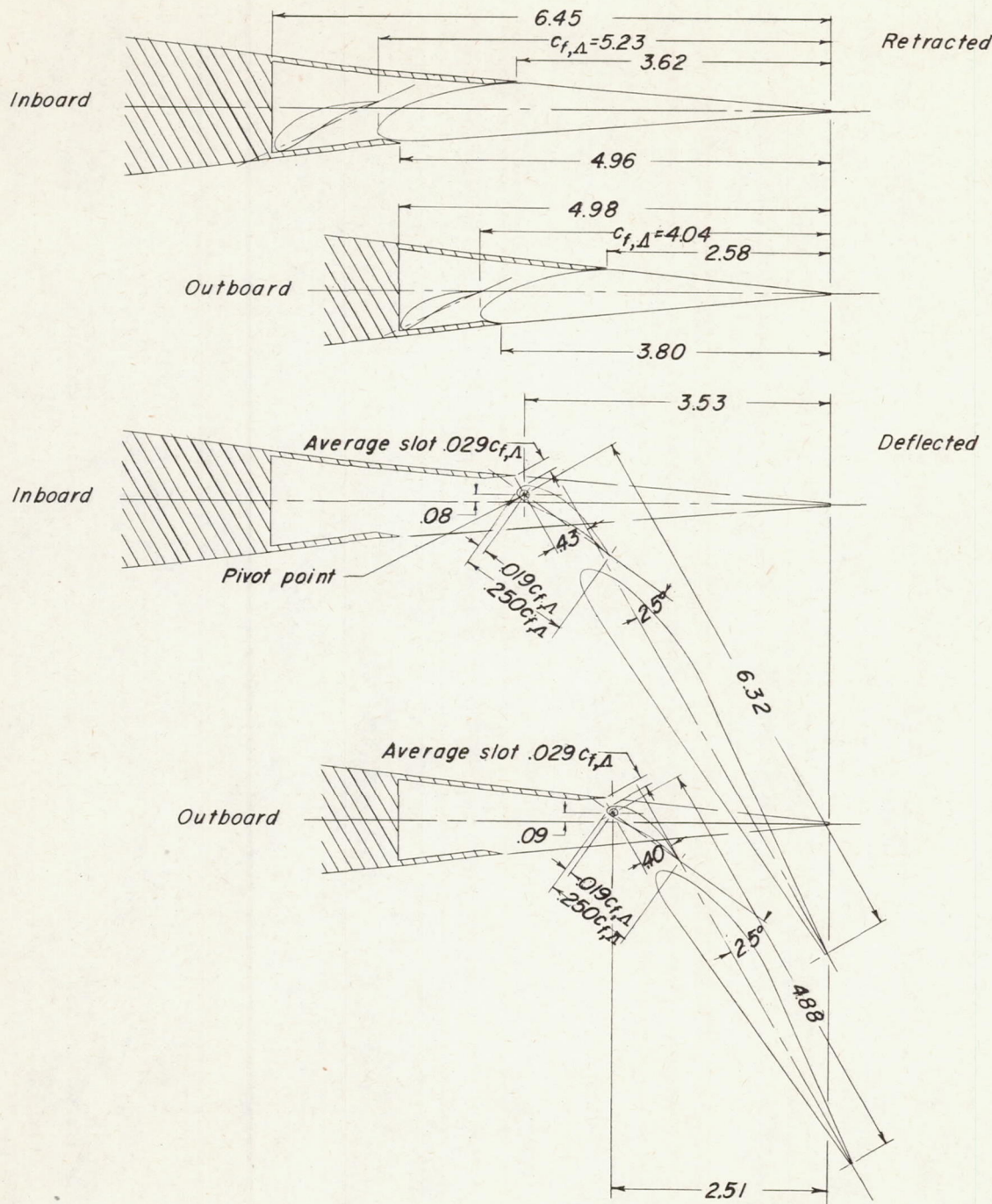
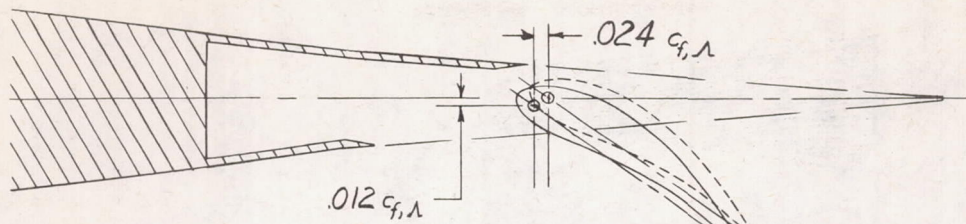
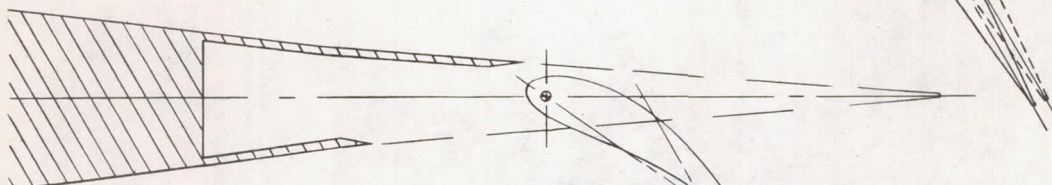
(b) Flap and $0.266c_f$ vane.

Figure 2.- Concluded.



(a) Pivot moved forward
and down.



(b) Flap moved forward.

Figure 3.- Alterations to basic flap and $0.500c_f$ vane configuration.

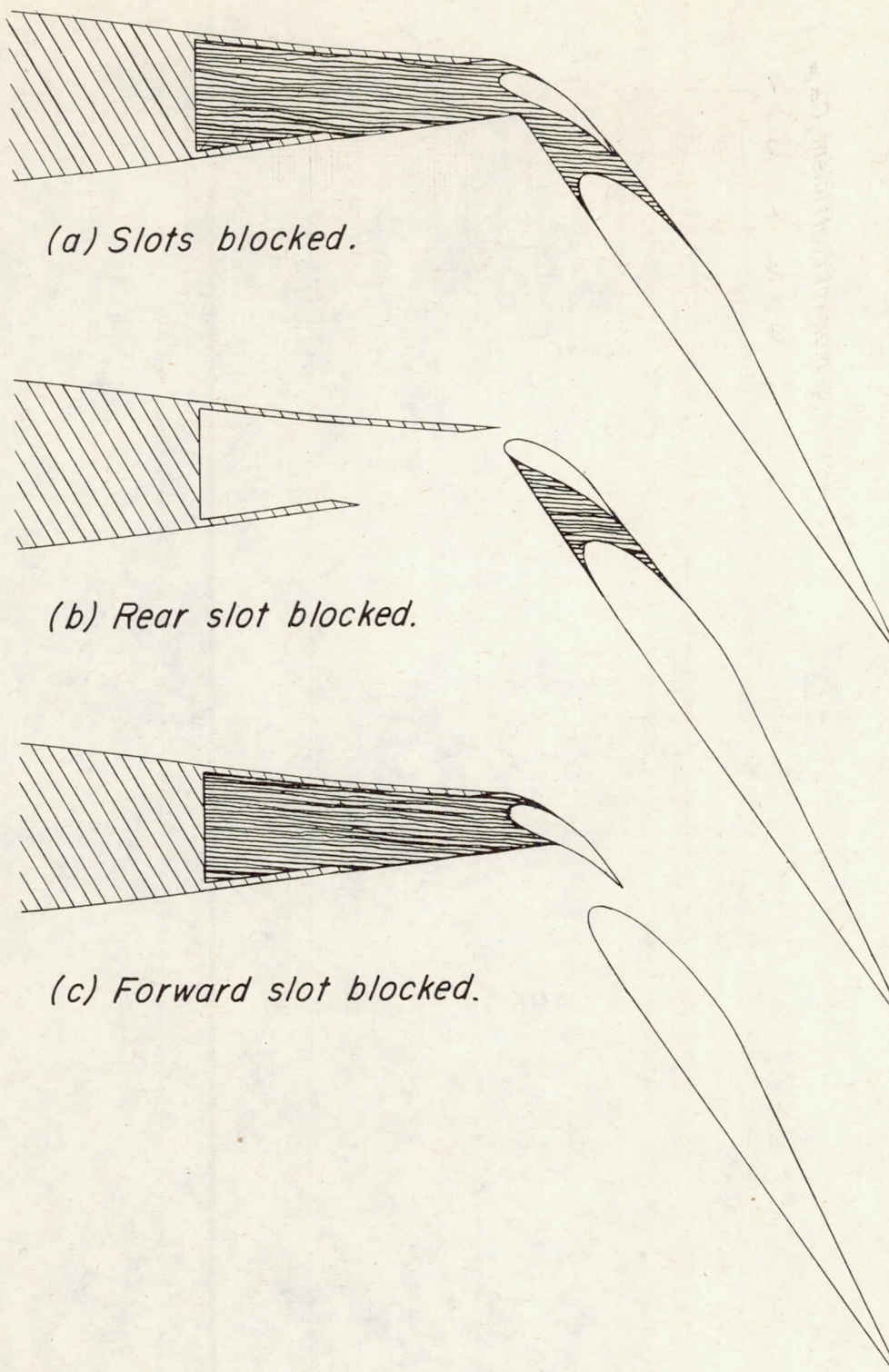


Figure 4.- Flaps with one or both slots blocked and faired.

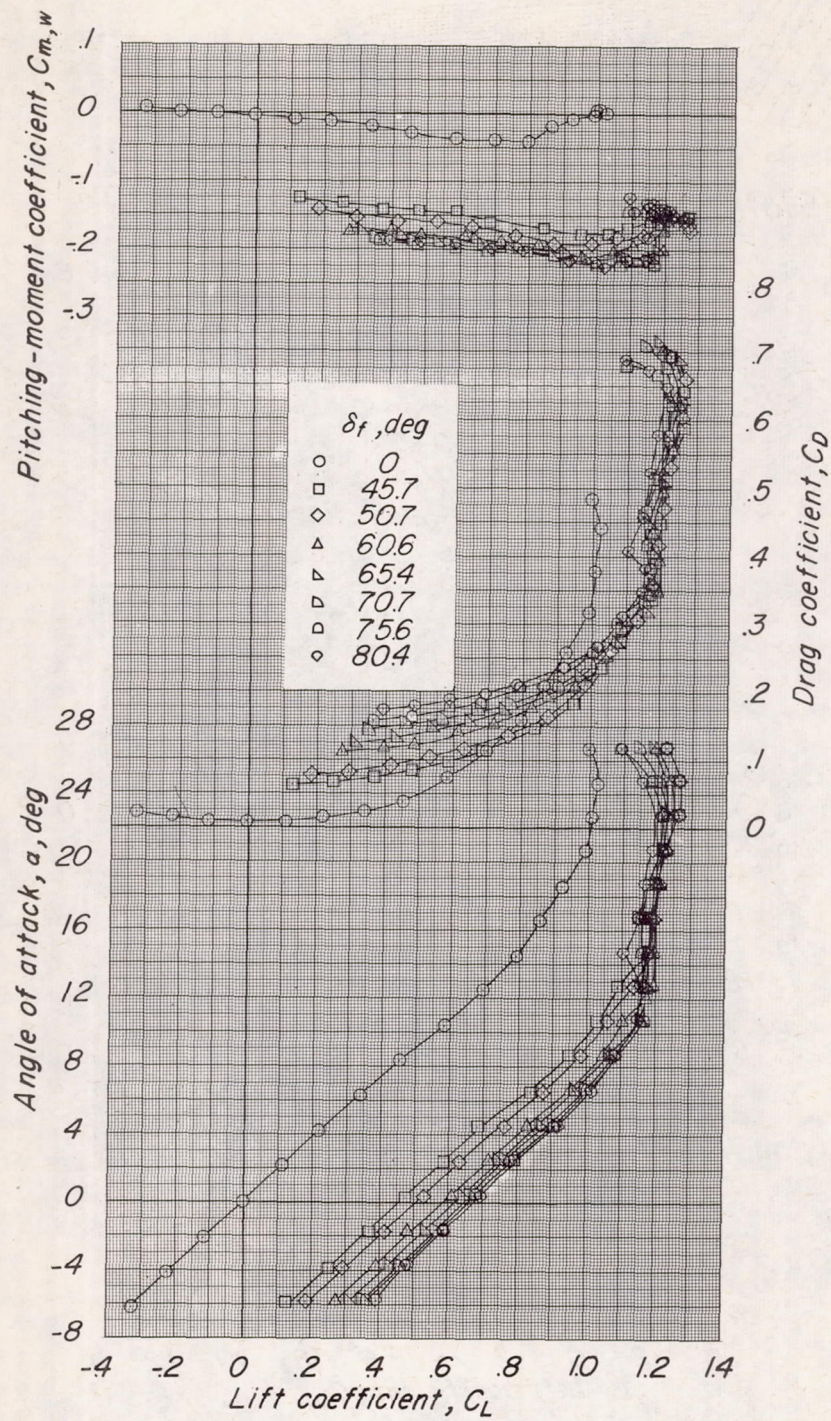


Figure 5.- Effect of deflection of the flap on the aerodynamic characteristics of the wing in pitch. 0.500c_f vane; double slotted.

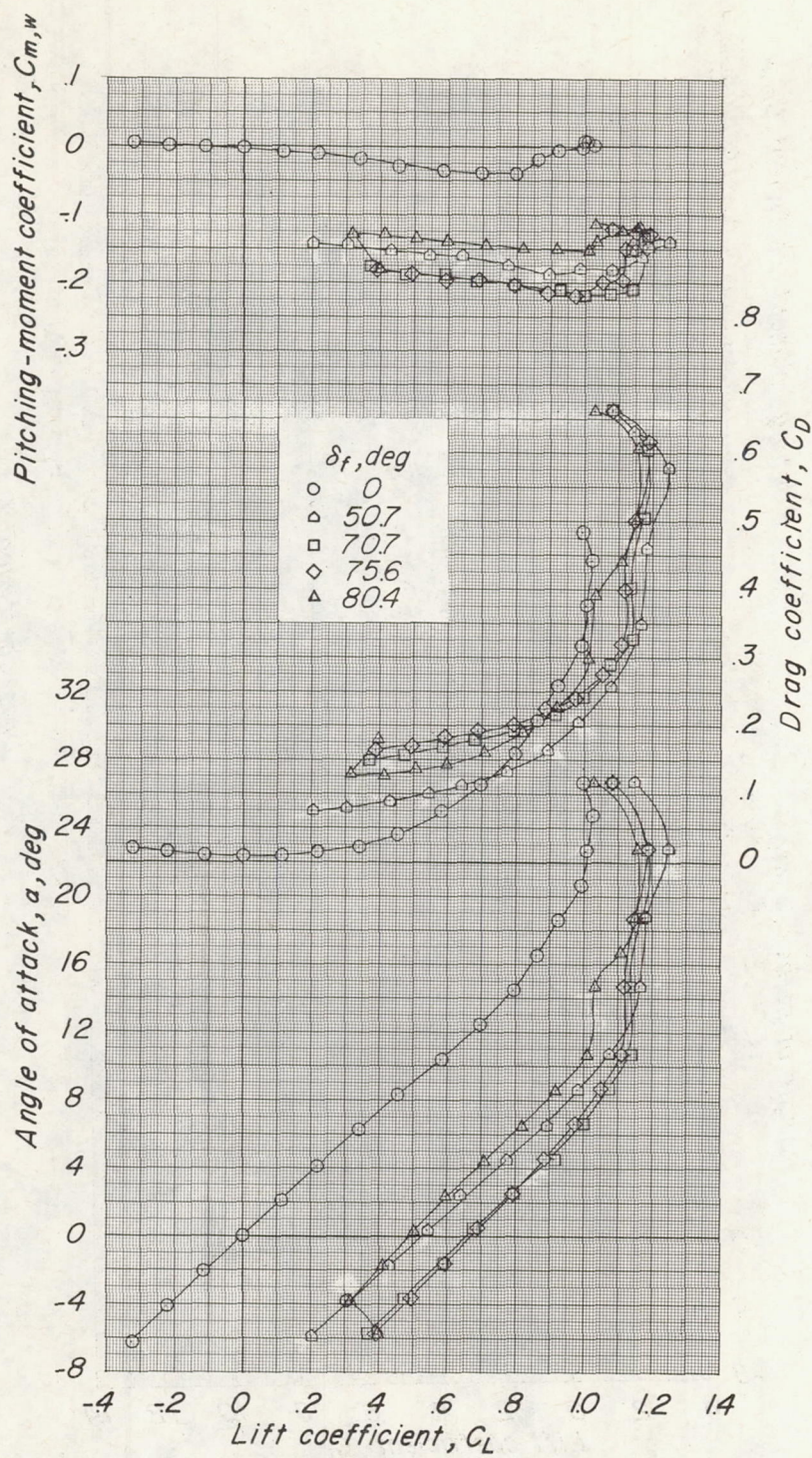


Figure 6.- Effect of deflection of the flap on the aerodynamic characteristics of the wing in pitch. 0.500c_f vane; rear slot blocked.

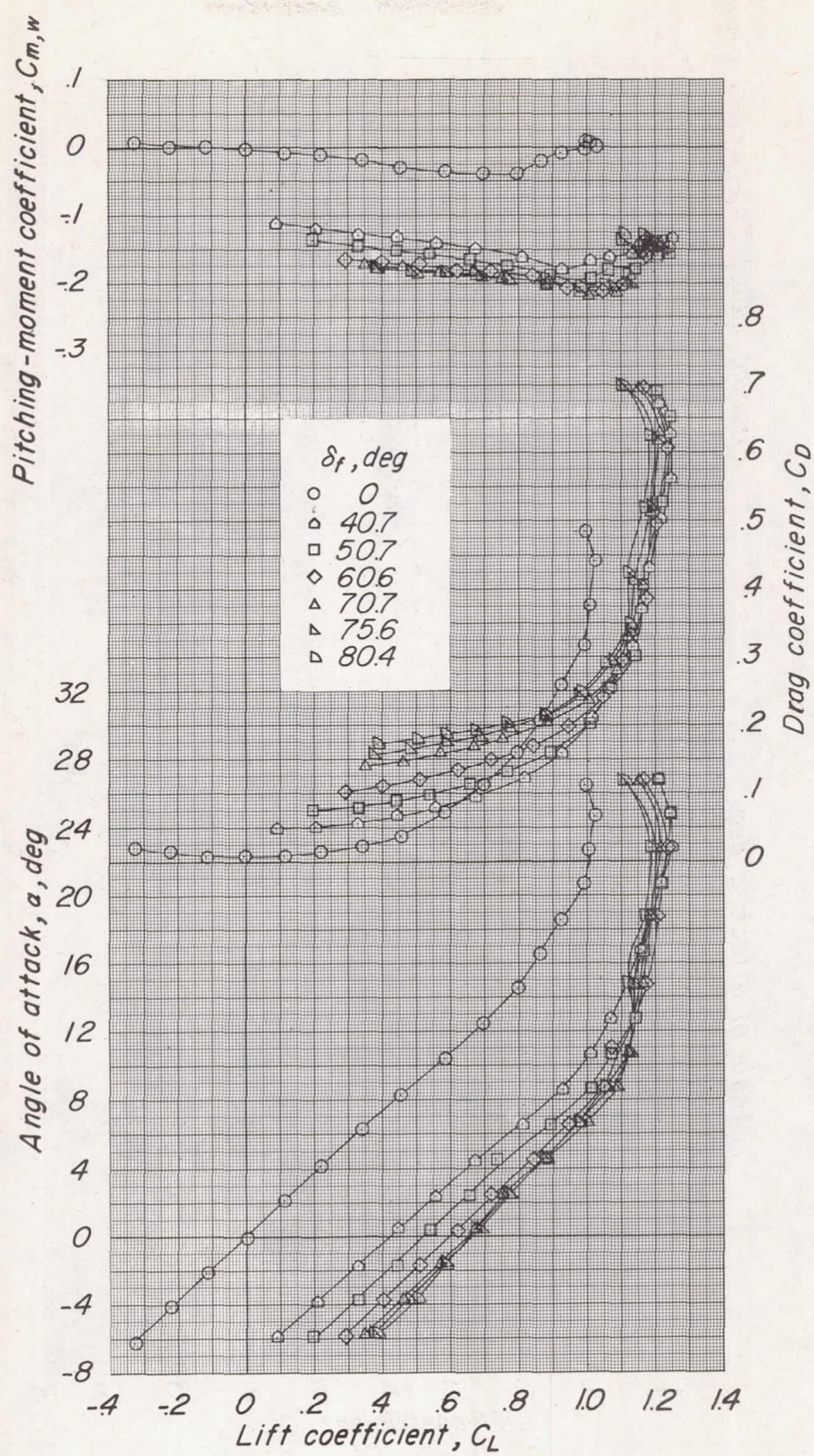


Figure 7.- Effect of deflection of the flap on the aerodynamic characteristics of the wing in pitch. $0.500c_f$ vane; forward slot blocked.

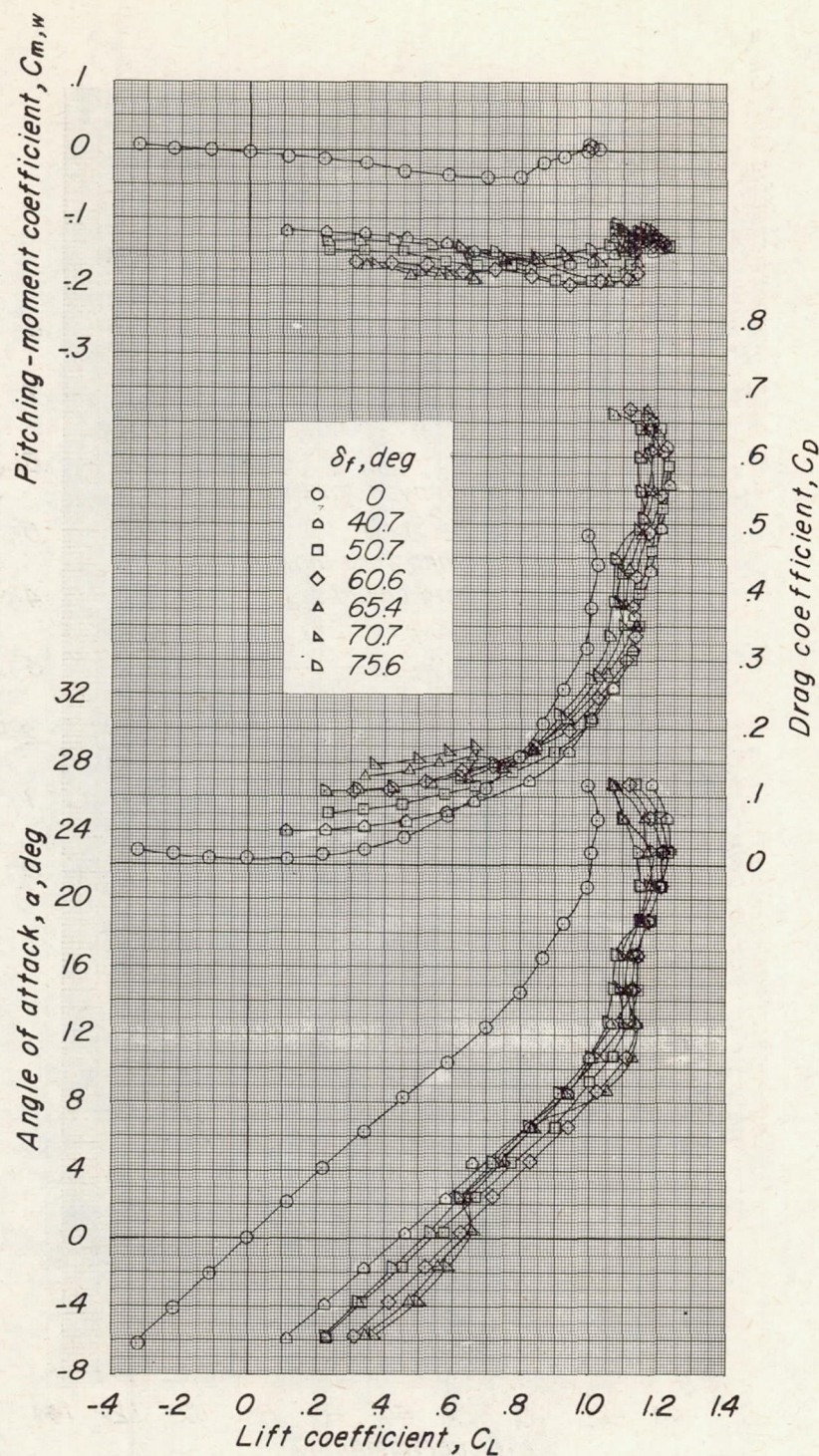


Figure 8.- Effect of deflection of the flap on the aerodynamic characteristics of the wing in pitch. 0.500 c_f vane; slots blocked.

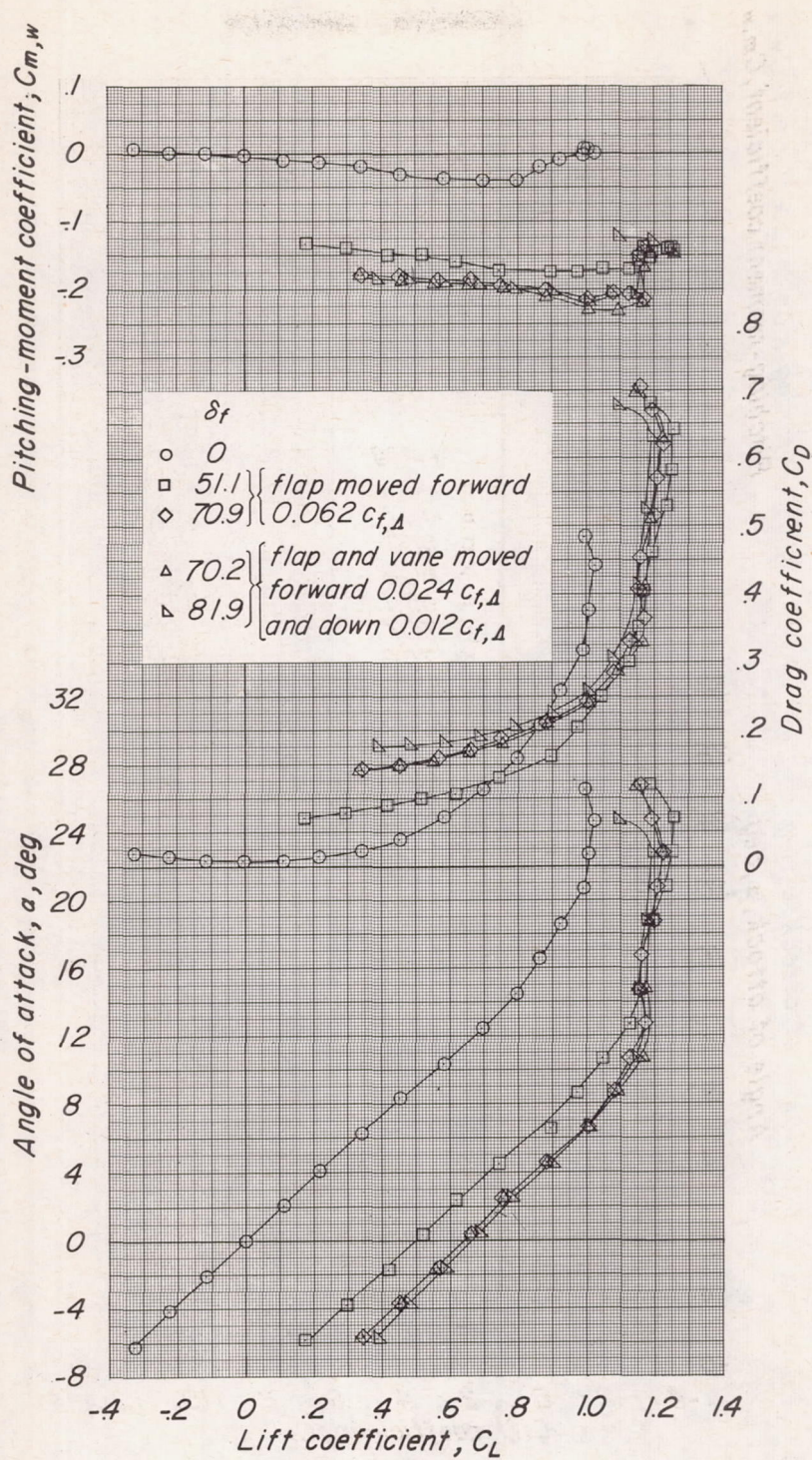


Figure 9.- Effect of location and deflection of the flap on the aerodynamic characteristics of the wing in pitch. 0.500 c_f vane; double slotted.

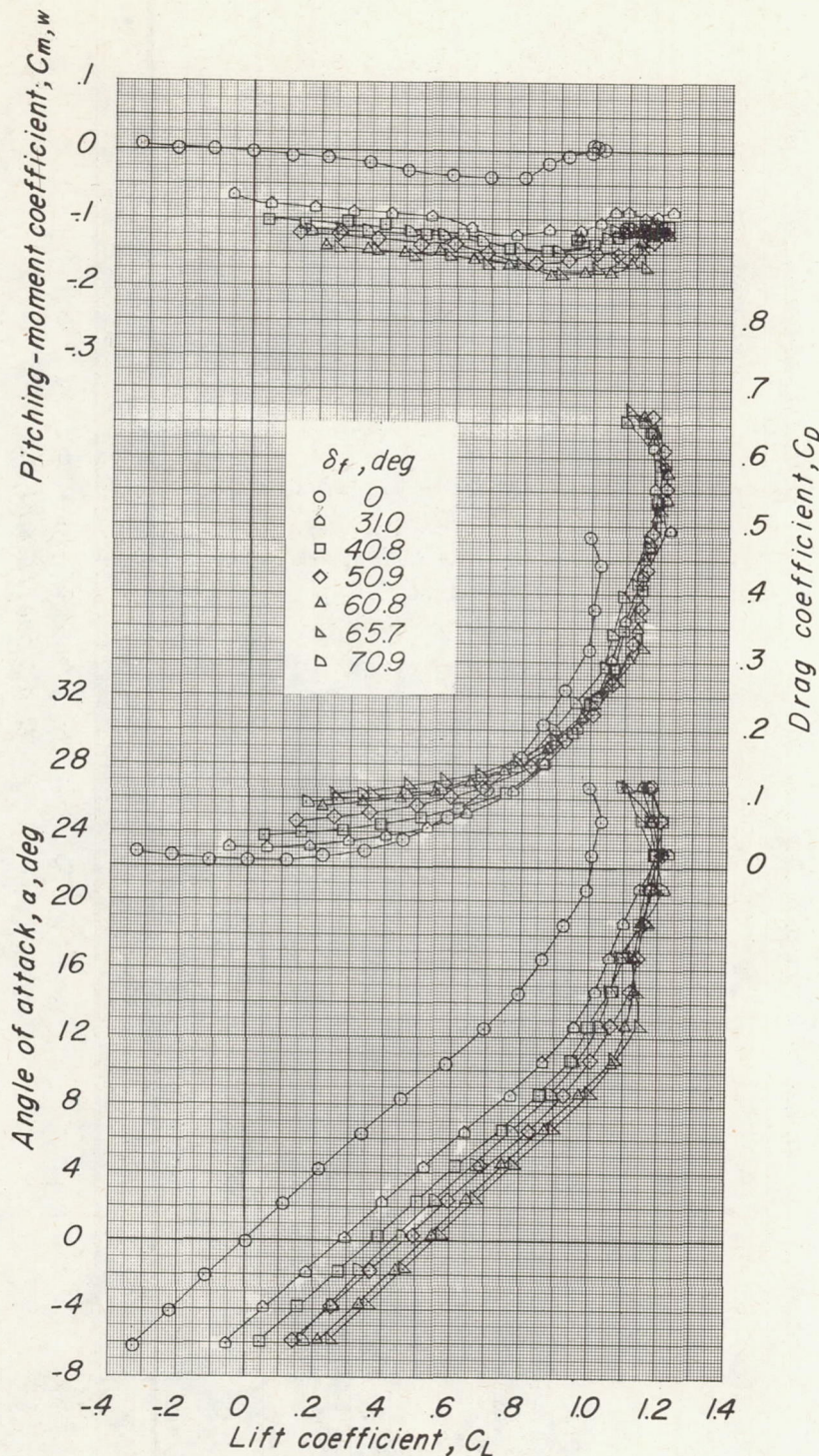


Figure 10.- Effect of deflection of the flap on the aerodynamic characteristics of the wing in pitch. $0.266c_f$ vane; double slotted.

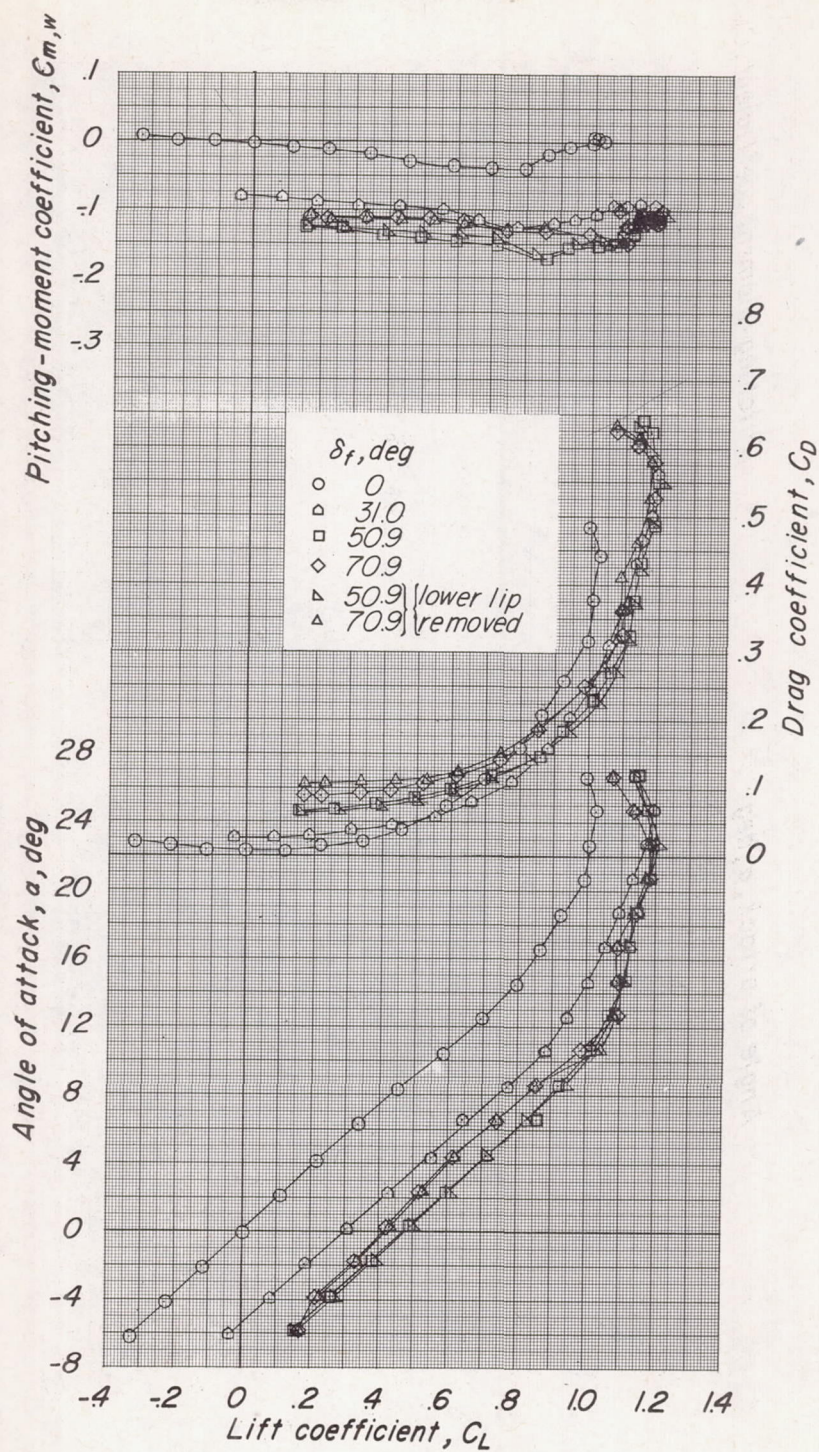


Figure 11.- Effect of deflection of the flap on the aerodynamic characteristics of the wing in pitch. 0.266c_f vane; rear slot blocked.

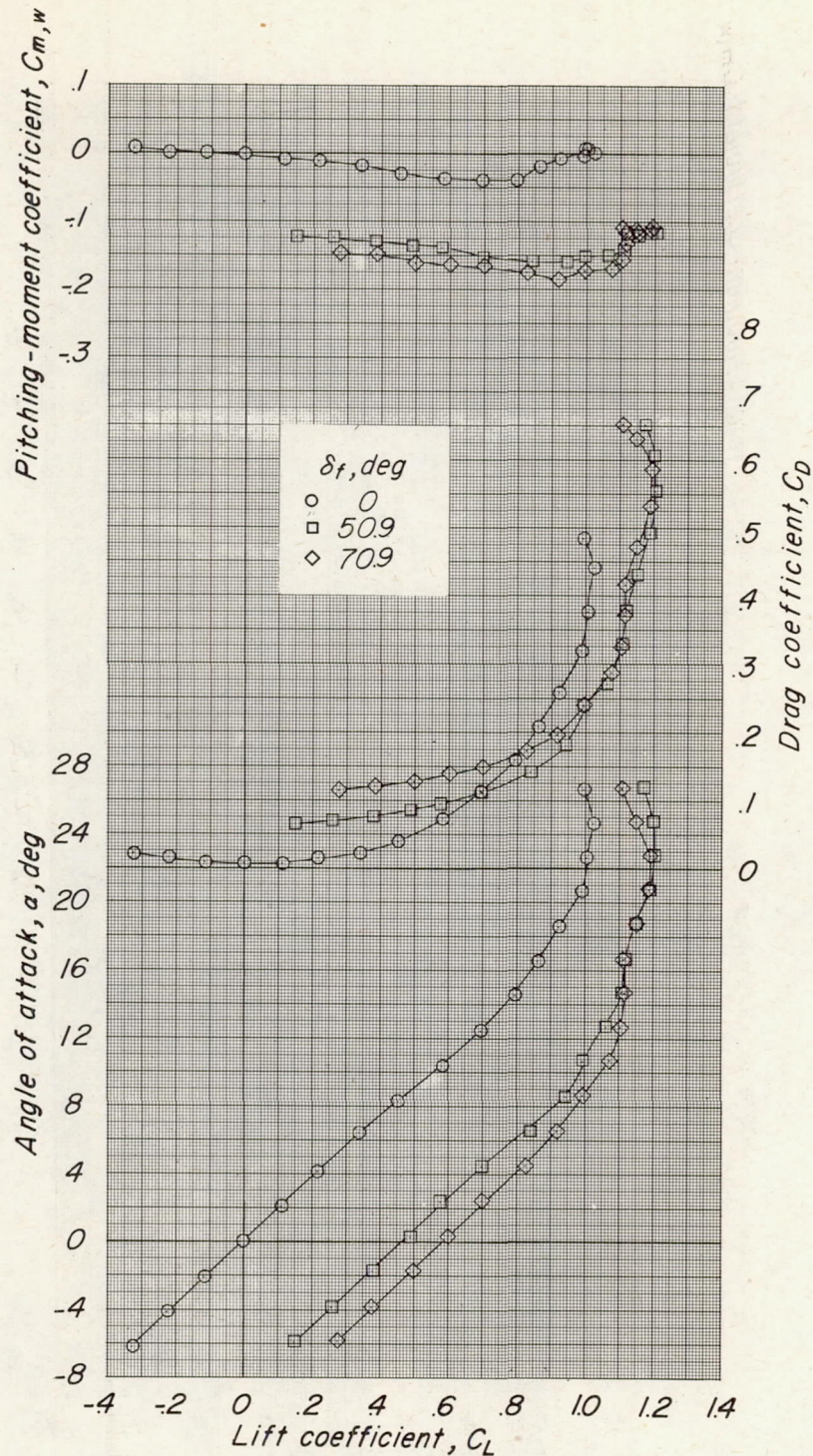


Figure 12.- Effect of deflection of the flap on the aerodynamic characteristics of the wing in pitch. 0.266c_f vane; forward slot blocked.

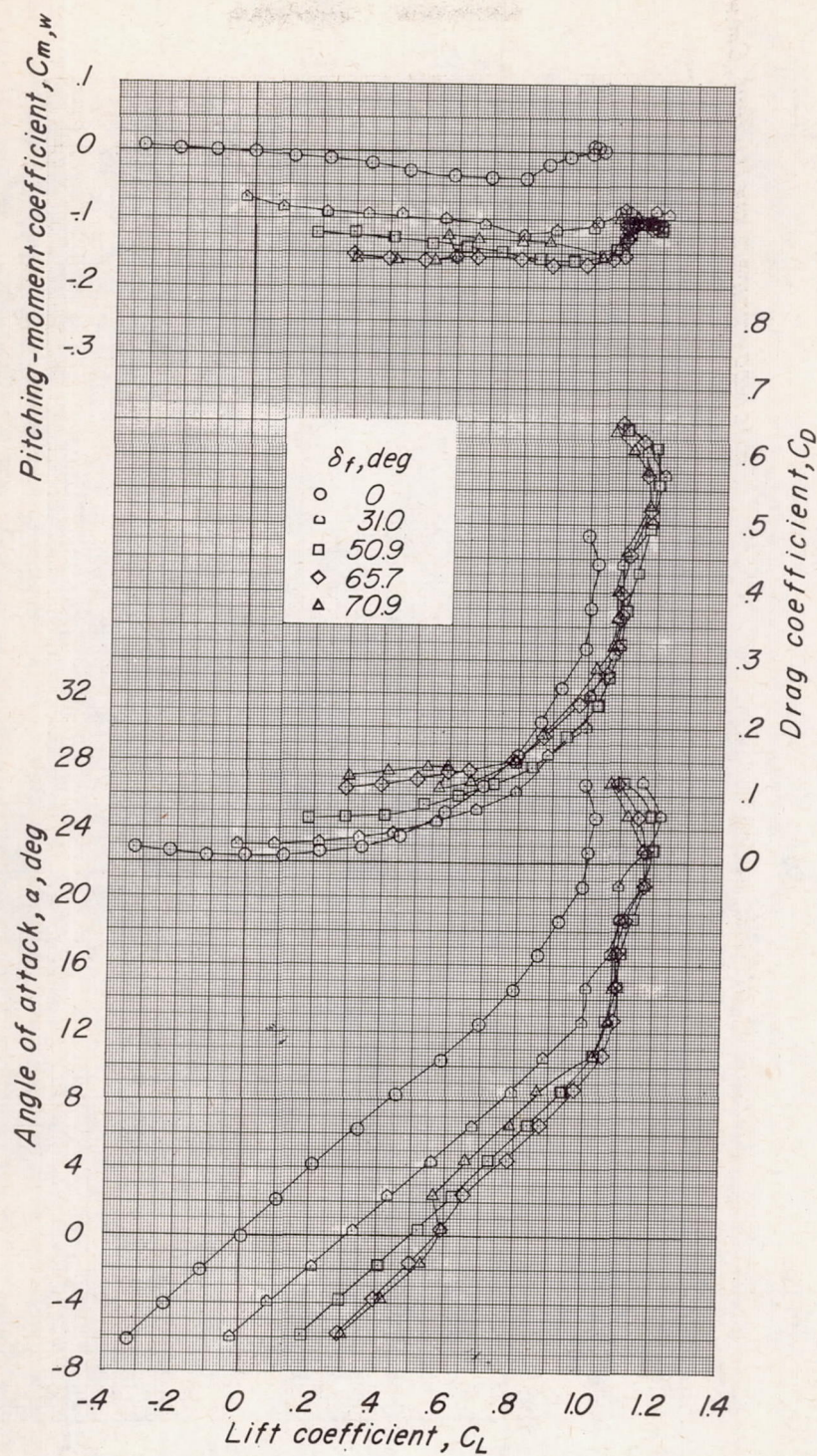


Figure 13.- Effect of deflection of the flap on the aerodynamic characteristics of the wing in pitch. 0.266 c_f vane; slots blocked.

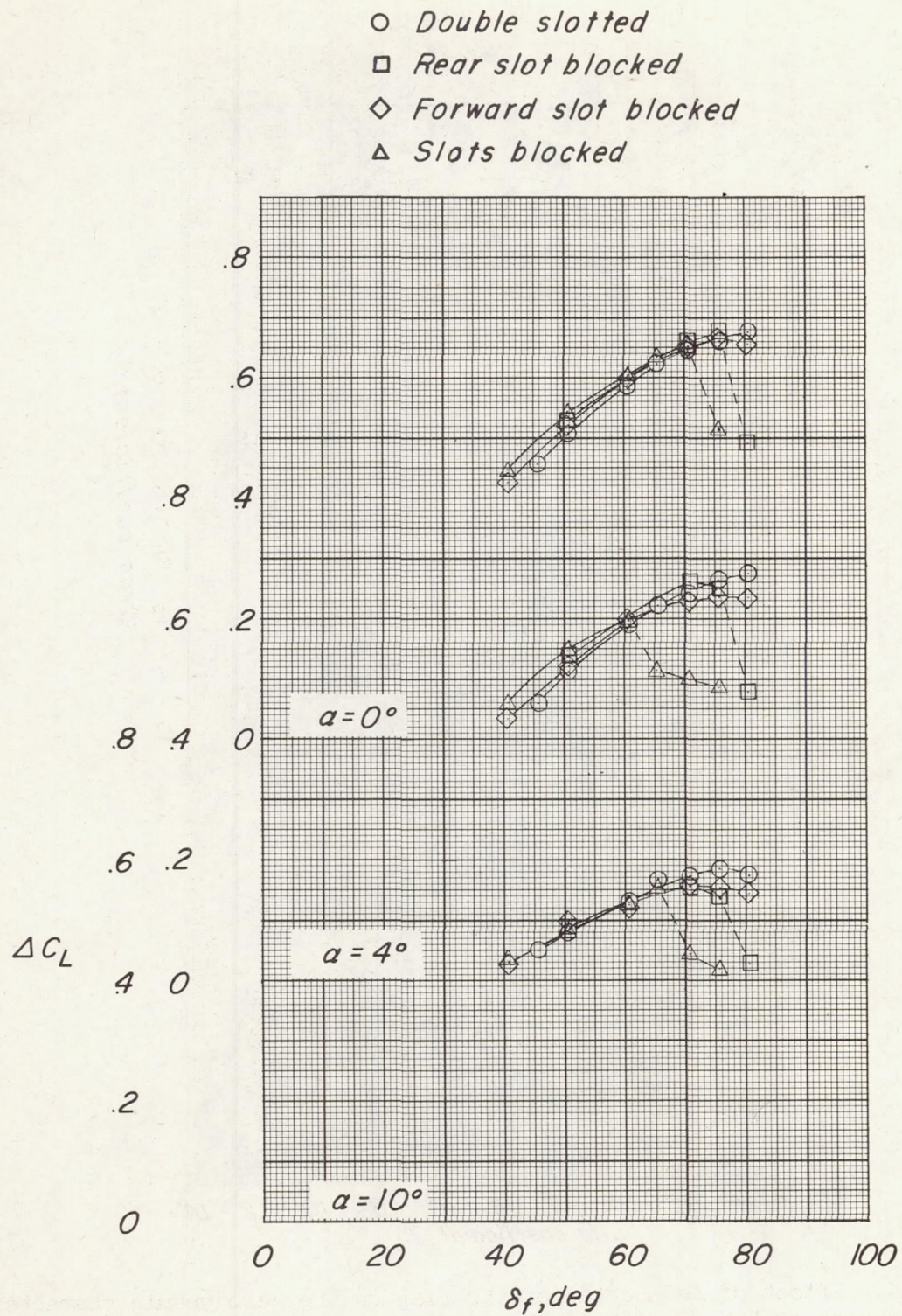


Figure 14.- Variation of lift increment with flap deflection. Flap and $0.500c_f$ vane.

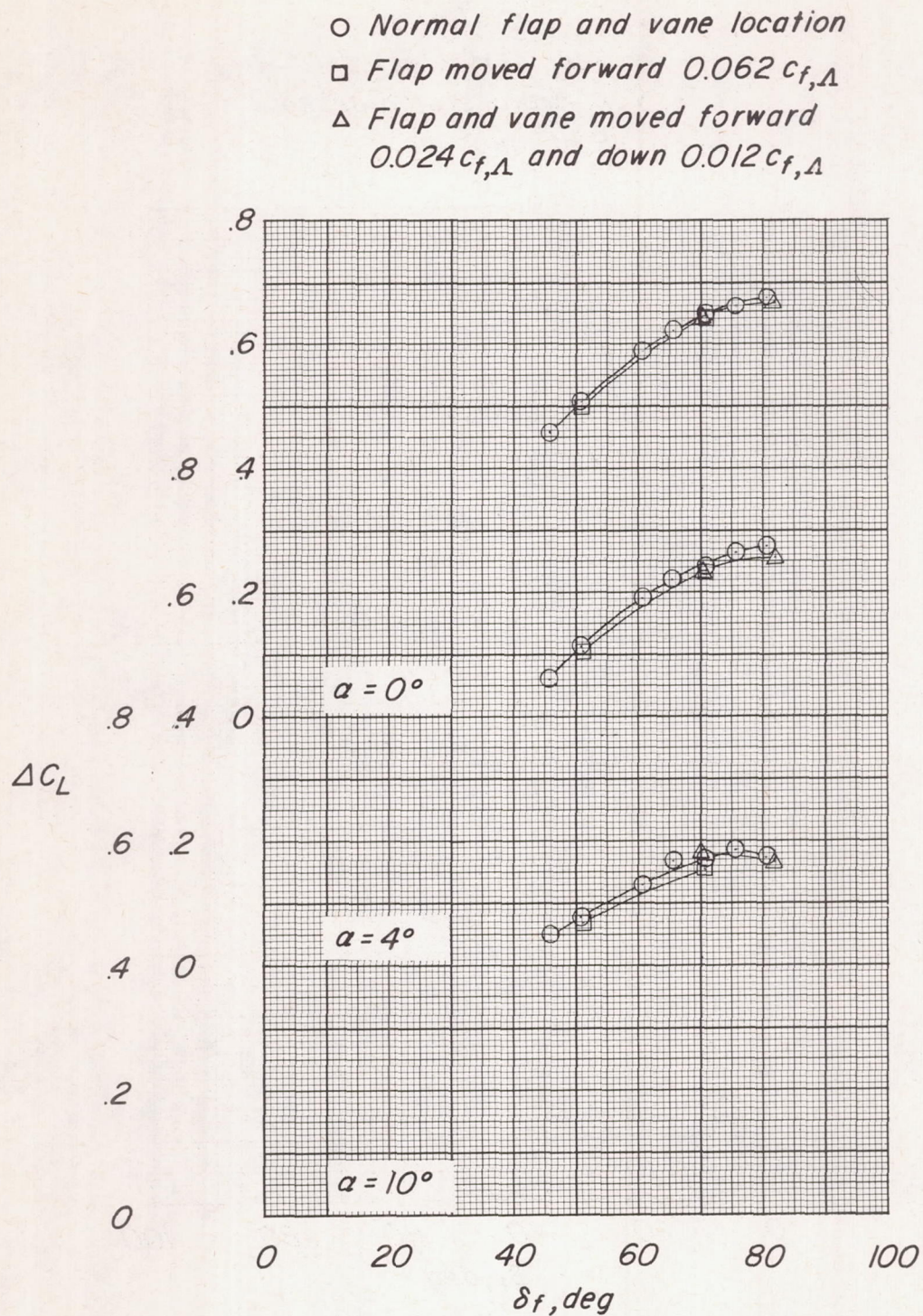


Figure 15.- Effect of change in flap geometry on the variation of lift increment with flap deflection. Double slotted flap; $0.500 c_f$ vane.

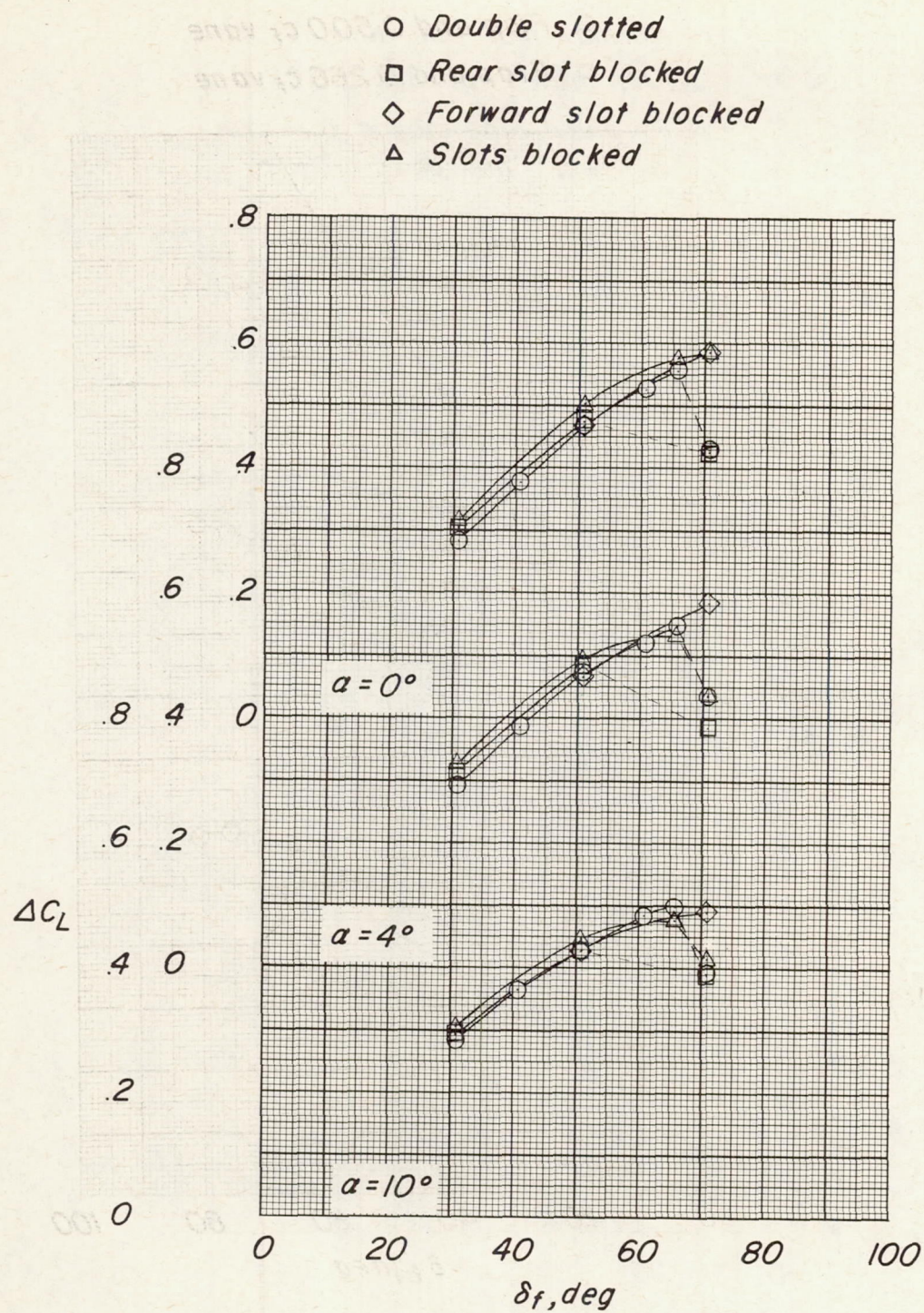


Figure 16.- Variation of lift increment with flap deflection. Flap and $0.266c_f$ vane.

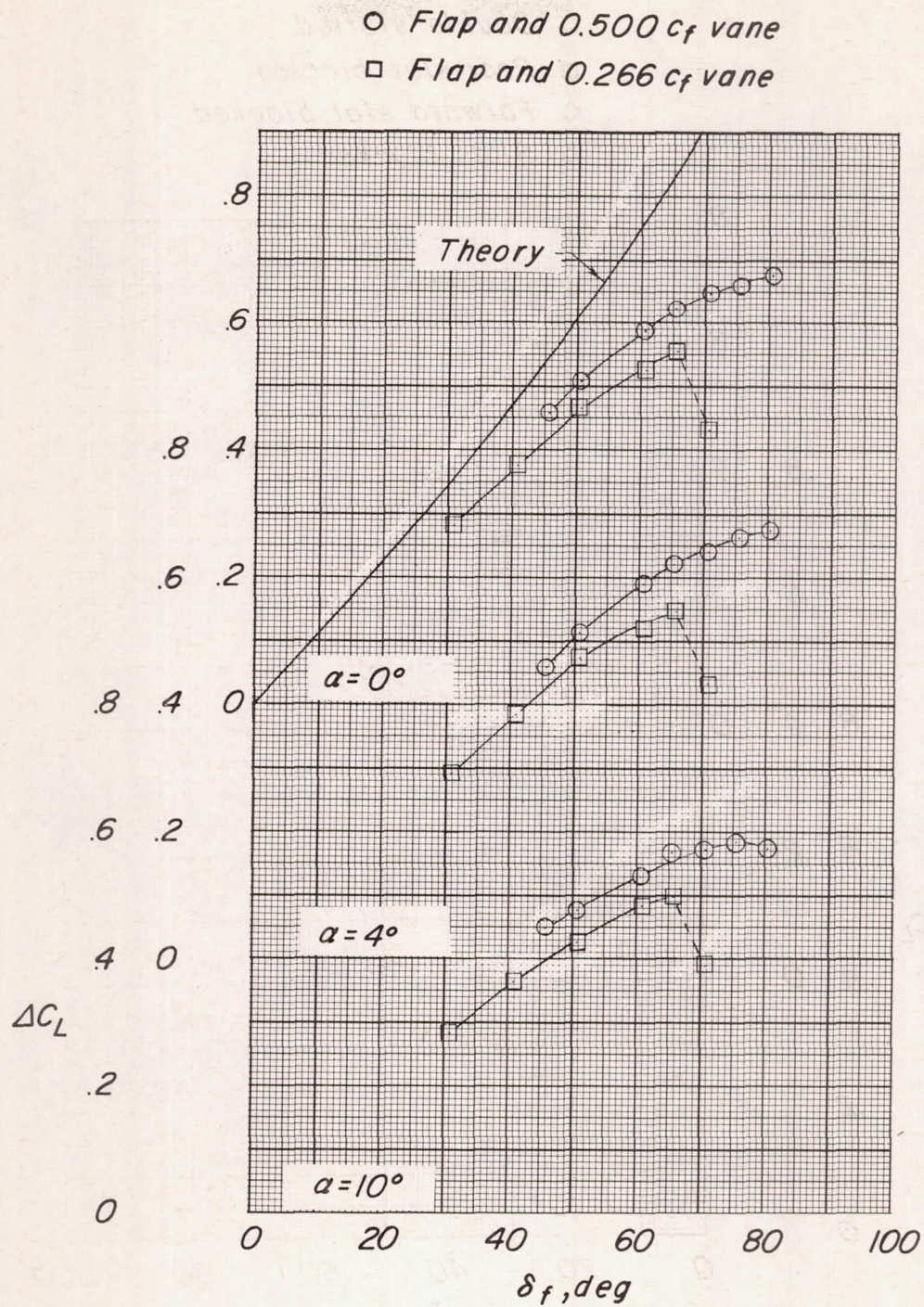


Figure 17.- Effect of vane size on the variation of lift increment with flap deflection. Double slotted flaps.

The amount of solar ultraviolet radiation reaching the Earth's surface depends on several factors:

1) The distance from the Sun. The closer the Sun, the greater the intensity of the radiation.

2) The angle of the Sun's rays relative to the Earth's surface.

3) The presence of clouds or other atmospheric

obstacles that can scatter or absorb the radiation.

4) The time of day and the season of the year.

5) The presence of ozone in the atmosphere.

6) The presence of other gases and particles in the atmosphere.

7) The presence of water vapor in the atmosphere.

8) The presence of dust and other particles in the atmosphere.

9) The presence of volcanic eruptions and other natural disasters.

10) The presence of man-made pollutants and other substances in the atmosphere.

11) The presence of the Sun's magnetic field and other factors.

12) The presence of the Earth's atmosphere and other factors.

13) The presence of the Sun's atmosphere and other factors.

14) The presence of the Earth's atmosphere and other factors.

15) The presence of the Sun's atmosphere and other factors.

16) The presence of the Earth's atmosphere and other factors.

17) The presence of the Sun's atmosphere and other factors.

18) The presence of the Earth's atmosphere and other factors.

19) The presence of the Sun's atmosphere and other factors.

20) The presence of the Earth's atmosphere and other factors.

21) The presence of the Sun's atmosphere and other factors.

22) The presence of the Earth's atmosphere and other factors.

23) The presence of the Sun's atmosphere and other factors.

24) The presence of the Earth's atmosphere and other factors.

25) The presence of the Sun's atmosphere and other factors.

26) The presence of the Earth's atmosphere and other factors.

27) The presence of the Sun's atmosphere and other factors.

28) The presence of the Earth's atmosphere and other factors.

29) The presence of the Sun's atmosphere and other factors.